How did the world's largest submarine fan in the Bay of Bengal grow and evolve at the subfan scale?

Chenglin Gong, Haiqiang Wang, Dali Shao, Hongping Wang, Kun Qi, and Xiaoyong Xu

ABSTRACT

Three individual subfan-growth cycles shown to stack up over time to form the Bengal Fan were recognized. Each of them underwent the following three main evolutionary stages. Stage 1, initial channel incision and amalgamation, was responsible for forming channel-complex sets (CCSs) with lateral trajectories and concomitant amalgamation with low aggradation. Stage 2, vertical channel aggradation and the resultant creation of intra-channel lows, was responsible for generating CCSs with vertical trajectories and concomitant organized stacking with high aggradation. Stage 3, channel avulsion and concomitant upstream propagation of lobes and crevasse splays, was responsible for developing crevasse splays and lobes. These three evolutionary stages constitute a single subfan-growth cycle (i.e., an individual single channel levee–lobe system). An abrupt shift of the channel levee position separates one subfan-growth cycle from the next. Different subfan-growth cycles stacked up over time gave rise to the world's largest submarine fan in the Bay of Bengal. The pinch-out of lobes and splays onto levees because of the channel avulsion during subfan evolutionary stage 3 created stratigraphiconlap traps with the potential for large hydrocarbon accumulations.

INTRODUCTION

Submarine channels are known as the primary conduits for the delivery of clastic detritus from continents to deepwater basins

Manuscript received May 3, 2019; provisional acceptance August 29, 2019; revised manuscript received January 21, 2020; revised manuscript provisional acceptance May 21, 2020; 2nd revised manuscript received June 1, 2020; 2nd revised manuscript provisional acceptance January 11, 2021; 3rd revised manuscript received January 29, 2021; 3rd revised manuscript provisional acceptance May 21, 2021; 4th revised manuscript received June 19, 2021; final acceptance August 9, 2021.
DOI:10.1306/02072219107

AUTHORS

CHENGLIN GONG ~ *State Key Laboratory of Petroleum Resources and Prospecting, China University of Petroleum (Beijing), Beijing, China; College of Geosciences, China University of Petroleum (Beijing), Beijing, China; chenglingong@cup.edu.cn*

Chenglin Gong is a professor at the College of Geosciences of the China University of Petroleum (Beijing). He obtained his Ph.D. in petroleum geosciences from the China University of Petroleum (Beijing) in 2014 and was a postdoctoral fellow working with Ronald J. Steel at the Jackson School of Geosciences of The University of Texas at Austin from 2014 to 2017. His research interests mainly focus on (1) source-to-sink sediment partitioning in deepwater basins, (2) sedimentology and stratigraphy of deepwater systems, and (3) the interplay of turbidity and contour currents. He is the corresponding author of this paper.

HAIQIANG WANG ~ *Chinnery Assets Limited, Yangon, Myanmar; wanghaiqiang@cal.net.mm*

Haiqiang Wang is an exploration manager at Chinnery Assets Limited, Yangon, Myanmar. He obtained his master's degree in 2007 from China University of Petroleum (Beijing) and a Ph.D. in 2010 from Research Institute of Petroleum Exploration and Development, China. His research interests focus on deepwater exploration.

DALI SHAO ~ *PetroChina Hangzhou Research Institute of Geology, Hangzhou, China; shaodl_hz@petrochina.com.cn*

Dali Shao is a senior geologist at the PetroChina Hangzhou Research Institute of Geology. He received his master's degree in 2007 from Chengdu University of Technology, China. His current research interests are petroleum geology, sedimentology, and seismic geomorphology.

HONGPING WANG ~ *PetroChina Hangzhou Research Institute of Geology, Hangzhou, China; wanghp_hz@petrochina.com.cn*

Hongping Wang is a senior geologist at the PetroChina Hangzhou Research Institute of Geology. He obtained his master's degree from China University of Petroleum (Beijing) in 2008. His research interests are petroleum accumulation and source rock evaluation.

KUN QI ~ *College of Geosciences, China University of Petroleum (Beijing), Beijing, China; qikun205@163.com*

Kun Qi is a Ph.D. candidate at the College of Geosciences of the China University of Petroleum (Beijing). He received a master's degree in geological resources and geological engineering from the Southwest Petroleum University in 2019. His research interests center on the sedimentology of deepwater channels and the source-to-sink sediment partitioning in deepwater basins.

XIAOYONG XU ~ *PetroChina Hangzhou Research Institute of Geology, Hangzhou, China; xuxy_hz@petrochina.com.cn*

Xiaoyong Xu is a senior geologist at the PetroChina Hangzhou Research Institute of Geology. He received his master's degree in 2008 from the China University of Geosciences (Beijing), China. He is mainly focused on deepwater sequence stratigraphy and sedimentology.

ACKNOWLEDGMENTS

This research was jointly funded by PetroChina Hangzhou Research Institute of Geology (No. 2019D-4309) and the Science Foundation of China University of Petroleum, Beijing (No. 2462020YXZZ020). We acknowledge Chinnery Assets Limited Company and Woodside for supporting our work and for offering us permission to publish this research. We are grateful to AAPG Editor Robert Merrill for editorial handling and to AAPG reviewers (Jennifer Pickering, Piret Plink-Bjorklund, and an anonymous reviewer) for their constructive comments, all of which significantly improved the overall quality of this research.

(e.g., Liu et al., 2013; Peakall and Sumner, 2015; Zhang et al., 2017). Deepwater lobes generally refer to sand-rich bodies accumulating in semiconfined or unconfined deepwater settings (e.g., Deptuck et al., 2008; Prélat et al., 2009). The progressive stacking of these two depositional elements builds submarine fans (Normark, 1970; Jobe et al., 2017; Bergmann et al., 2020). Submarine fans have been the focus of extensive research since their discovery in the 1950s (Menard, 1955; see also Shanmugam, 2016; Deptuck and Sylvester, 2017 for a recent review). This is largely because submarine fans (1) are the volumetrically largest sediment accumulations on Earth (e.g., the Bengal Fan as documented in this case) (Covault, 2011; Liu et al., 2013; Deptuck and Sylvester, 2017; Zhang et al., 2017); (2) represent the second largest global sink of the atmospheric carbon dioxide (Galy et al., 2008); (3) can be petroliferous reservoirs (e.g., Richards et al., 1998; Pettingill and Weimer, 2002; Deptuck and Sylvester, 2017); and (4) preserve critical paleoclimatic and paleoceanographic information (Prélat et al., 2010; Covault, 2011; Picot et al., 2016). Therefore, it is essential to understand the depositional elements and growth and evolution patterns of submarine fans (Shanmugam, 2016; Deptuck and Sylvester, 2017).

Previous studies have suggested that the complex interplay of allogenic and autogenic processes determine the evolution and growth of submarine fans (e.g., Prélat et al., 2010; Dorrell et al., 2015). The results of allogenic processes (e.g., eustatic fluctuations, climatic changes, and sediment supply regimes, etc.) and autogenic processes (e.g., adjustments toward an equilibrium gradient) on submarine fan evolution and growth have been extensively documented (e.g., Mutti and Normark, 1987; Lopez, 2001; Covault and Romans, 2009; Covault, 2011; Dorrell et al., 2015; Covault et al., 2016; Picot et al., 2016). However, research on modern submarine fan systems (e.g., the Amazon Fan documented by Lopez, 2001; the Zaire Fan documented by Picot et al., 2016; and the intraslope submarine fan on the western Niger Delta slope documented by Jobe et al., 2017) and their ancient analogues (e.g., the Carboniferous Ross Sandstone highlighted by Pyles, 2008; the Permian Skoorsteenberg Formation highlighted by Prélat et al., 2009; and the middle to upper Pleistocene lower Bengal Fan by Bergmann et al., 2020) have revealed that the evolution and growth patterns of submarine fans are far from being well understood.

Using commercially acquired three-dimensional (3-D) seismic data sets and regional two-dimensional (2-D) seismic lines from the world's largest submarine fan in the Bay of Bengal (Figure 1), the current study attempts to (1) document architectural styles and repetitive growth patterns of the Bengal Fan at the subfan scale (i.e., individual channel levee–lobe systems) and (2) characterize stratigraphic relationships of individual Bengal channel levee–lobe systems (i.e., subfans). Results from the

present study help obtain a better understanding of the initiation, growth, and decay of the world's largest detrital accumulation at the subfan scale.

GEOLOGICAL BACKGROUND OF THE STUDY AREA

Ganges–Brahmaputra–Bengal Source-to-Sink Systems

The study area lies in the Rakhine Basin along the eastern fringe of the Bay of Bengal, which is known as the terminus of the world's largest source-to-sink systems (i.e., Ganges–Brahmaputra–Bengal sediment-routing systems) (Figure 1). The Himalayan-sourced Ganges–Brahmaputra river systems have a contributing drainage area of greater than 2.0×10^6 km^2. Ganges–Brahmaputra river systems deliver terrestrial sediments from the Himalayas down to the Bay of Bengal (>4000-m water depth) (Kuehl et al., 2005; Pickering et al., 2014; Romans et al., 2016; Blum et al., 2018) (Figure 1). Their catchment areas have an average denudation rate that is 12 times higher than the global average denudation rate (Islam et al., 1999). The Ganges–Brahmaputra–Bengal sediment-routing system annually delivers more than 1 Gt of sediments to the delta plain in India and Bangladesh: an estimated 70% of the total modern load is from the Brahmaputra, whereas 30% derives from the Ganges (Goodbred, 2003; Blum et al., 2018).

The transfer of terrestrial sediments from the shelf down to Bengal deepwater is guided through the Swatch of No Ground Canyon (e.g., Kudrass et al., 1998; Schwenk et al., 2005; Rogers and Goodbred, 2010). The Swatch of No Ground Canyon has cut headward across the broad Bangladesh shelf for nearly 150 km with its head in water depth of only 38 m (Sweet and Blum, 2016). Such proximity between the shorelines and canyon heads has yielded and maintained a direct connection between subaerial and submarine segments of the Ganges–Brahmaputra–Bengal sediment-routing system (see also Sweet and Blum, 2016). The proximity between shorelines and canyon heads, together with westward-flowing, along-shelf currents (Kuehl et al., 2005), cyclones (Michels et al., 1998), storms (Kudrass et al., 1998), tidal currents (Rogers and Goodbred, 2010), earthquakes (Michels et al., 2003), and/or monsoonal pulses (Weber et al., 1997), have facilitated the delivery of nearly one-third of the sediment load of the Ganges River into the Bay of Bengal, resulting in the world's largest submarine fans (2500 to 3000 km in length, 830 to 1430 km in width, 2.8 to 3.0×10^6 km^2 in area, 12.5×10^6 km^3 in volume, and 2.88×10^{16} t in the mass of sediments) (e.g., Goodbred and Kuehl, 1999; Curray et al., 2002; Goodbred, 2003; Kuehl et al., 2005) (Figure 1).

The present-day geometry of the Bengal Fan is a complex of different channel levee–lobe systems, each of which has been referred to as a "subfan" (Curray et al., 2002) and shows a considerable amount of lateral shifting. However, it is believed that only a single subfan was active at a given interval of geological time (Curray et al., 2002; Bastia et al., 2010). A gradient-based tripartite division of the Bengal Fan into upper, middle, and lower subenvironments has been proposed by Curray et al. (2002). The study area is in the Rakhine Basin in the northeastern fingers of the middle Bengal Fan. Three discrete channel levee–lobe systems (i.e., subfans 1–3 in Figure 2A, B) are well imaged by commercial 2-D and 3-D seismic data utilized in this study. Among them, subfan 2 is the focus of the current study (Figures 2A, B; 3).

Tectonostratigraphic Evolution of the Bengal Fan

The initiation of the Bengal Fan was induced by the collision between the Eurasian and Indian plates and their associated uplift of the Himalayas in the early Eocene (Yin, 2006; Bastia et al., 2010; Ma et al., 2020). The Bengal Fan underwent two main stages of the tectonostratigraphic evolution since its initiation, including a rift stage from the early Eocene to middle Miocene and a postrift stage from the late Miocene to Holocene (Curray et al., 2002; Bastia et al., 2010). Successions formed during these two tectonostratigraphic evolutionary stages are bounded at their bases by two basin-wide unconformities dated as early Eocene and late Miocene, respectively (Krishna et al., 2009; Yang and Kim, 2014). The chronologically older unconformity dated circa 55 Ma (i.e., early Eocene) is recognized as the Paleocene–Eocene hiatus by Curray et al. (2003) and is traceable throughout the Bengal Fan. This lower Eocene unconformity marks the initiation of Indian collision, Himalayan uplift, and Bengal Fan sedimentation.

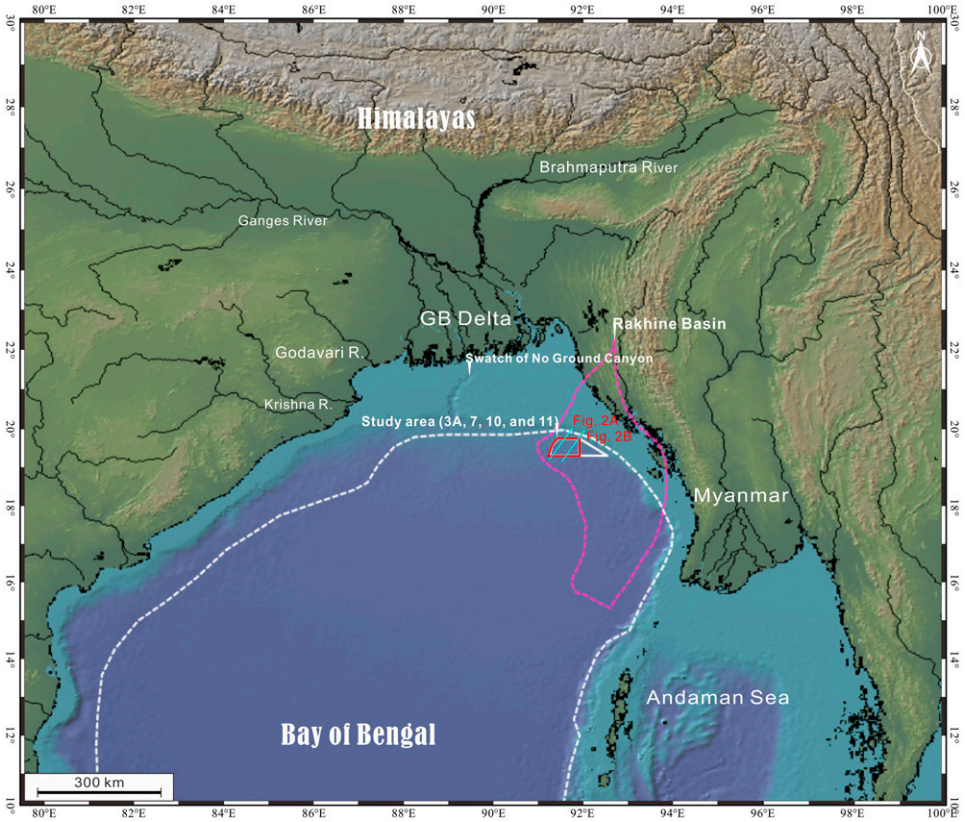

Figure 1. Regional map of the Bay of Bengal showing geographic context of the study area plan-view locations of seismic lines shown in Figure 2 (labeled). Flattened horizontal seismic amplitude slices shown in Figure 3A and horizontal route-mean-square–attribute slices presented in Figure 7 cover the full three-dimensional area marked by the red box. GB = Ganges–Brahmaputra; R. = River.

The chronologically younger unconformity dated circa 8 Ma (i.e., late Miocene) was generated by the intraplate deformation of the oceanic lithosphere (Krishna et al., 2009; Yang and Kim, 2014; Ma et al., 2020). The late Miocene to present deposition in the Bengal Fan was significantly influenced by the collision between the Eurasian and Indian plates (Curray et al., 2002; Bastia et al., 2010; Ma et al., 2020). Seismically well-imaged channel levee–lobe systems were well developed during the postrift period from the late Miocene to Holocene, and are the focus of the present study (i.e., subfans 1–3 seen on Figures 2, 3).

DATABASE AND METHODOLOGY

The 2-D and 3-D Seismic Reflection Data

The primary data set utilized in this study is 1000 km^2 of 3-D seismic data, tied to regional 2-D seismic lines, acquired from the middle Bengal Fan (Figure 1). The Bengal 3-D seismic data have a bin size spacing of 25 m (in-line) by 12.5 m (cross-line). Both 2-D and 3-D seismic data sets have a sampling interval of 4 ms and have been processed using a prestack hybrid migration algorithm. They have a dominant frequency of 20 to 30 Hz for the study interval of interest, yielding a vertical resolution of 12.5 to 18.75 m (λ/4) (λ is wavelength) and detection of 2 to 3 m (λ/25). Both 2-D and 3-D seismic data were displayed using Society of Exploration Geophysicists negative standard polarity. A positive reflection coefficient corresponds to an increase in acoustic impedance and is represented by a positive reflection event (Figures 2–6). They were displayed using a red–white–black color bar, where the low-impedance reservoir top is displayed as a peak (red) (Figures 2–6).

Seismic Stratigraphy and Geomorphology

The present study integrates classical 2-D seismic stratigraphic analysis with the 3-D geomorphology

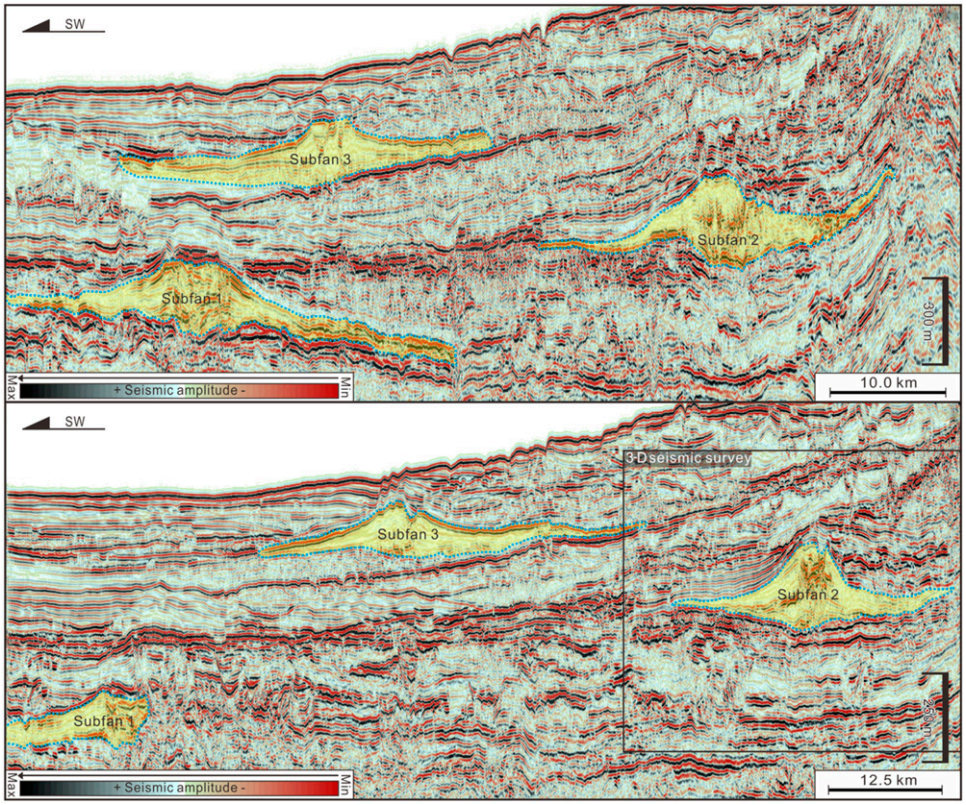

Figure 2. Regional two-dimensional seismic lines (see line locations in Figure 1) from the Bay of Bengal depicting the occurrence of subfans 1–3. Among these three shown subfan-growth cycles, subfan-growth cycle 2 (black box labeled 3-D seismic survey in (B)) is the focus of the present study. Note that these three subfan-growth cycles abruptly shifted and stacked up through time, giving rise to the world's largest submarine fan in the Bay of Bengal. 3-D = three-dimensional; Max = maximum; Min = minimum.

approach, through which seismic stratigraphy and geomorphology of the Bengal channel levee–lobe systems were graphically delineated. The 3-D amplitude volumes and root-mean-square (RMS)-attribute cubes utilized in this study were produced through two main steps (Figures 3A, 7). The first step was to flatten the Bengal 3-D seismic amplitude volumes using the seismic surface of T_{ft} shown in Figure 3B as the hanging horizon (0 ms). The second step was to produce 3-D RMS-attribute volumes using the flattened seismic amplitude volumes. The 3-D amplitude and RMS-attribute cubes, coupled with 2-D seismic transects, were used to delineate both plan-view and cross-sectional seismic manifestations of the Bengal subfan 2 (Figures 2, 3). Channel-complex sets (CCSs), which record individual cycles of channel cutting, filling, avulsion, and abandonment, are commonly the smallest channel form resolvable in seismic reflection data (Gong et al., 2021). This study is based mainly on seismic data sets and thereby has a focus at the scale of CCSs.

In addition, Bengal seismic data sets are used to quantify morphometric properties, architectural styles, and growth patterns of the studied Bengal channel levee–lobe systems.

First, bankfull geometries of the studied channels have been quantified in terms of (1) bankfull channel width (*B*)—measured as the maximum horizontal distance between channel banks (Figure 3B); (2) bankfull channel depth (*H*)—measured as the maximum vertical relief from the channel base in the axial zone to the channel bank (Figure 3B); and (3) aspect ratio (*B/H*)—computed by dividing *B* by *H*. Second, cross-sectional geometries of levees coeval with the studied channels were quantified in terms of (1) levee width (*W*)—measured as the maximum horizontal distance from the levee crest to its lateral termination (i.e., the intersection between the levee base and the upper bounding surface of the levees) (Figure 3B); (2) levee thickness (*T*)—measured as the maximum vertical distance from the levee crest to the levee base (Figure 3B); and (3) width-to-thickness ratio

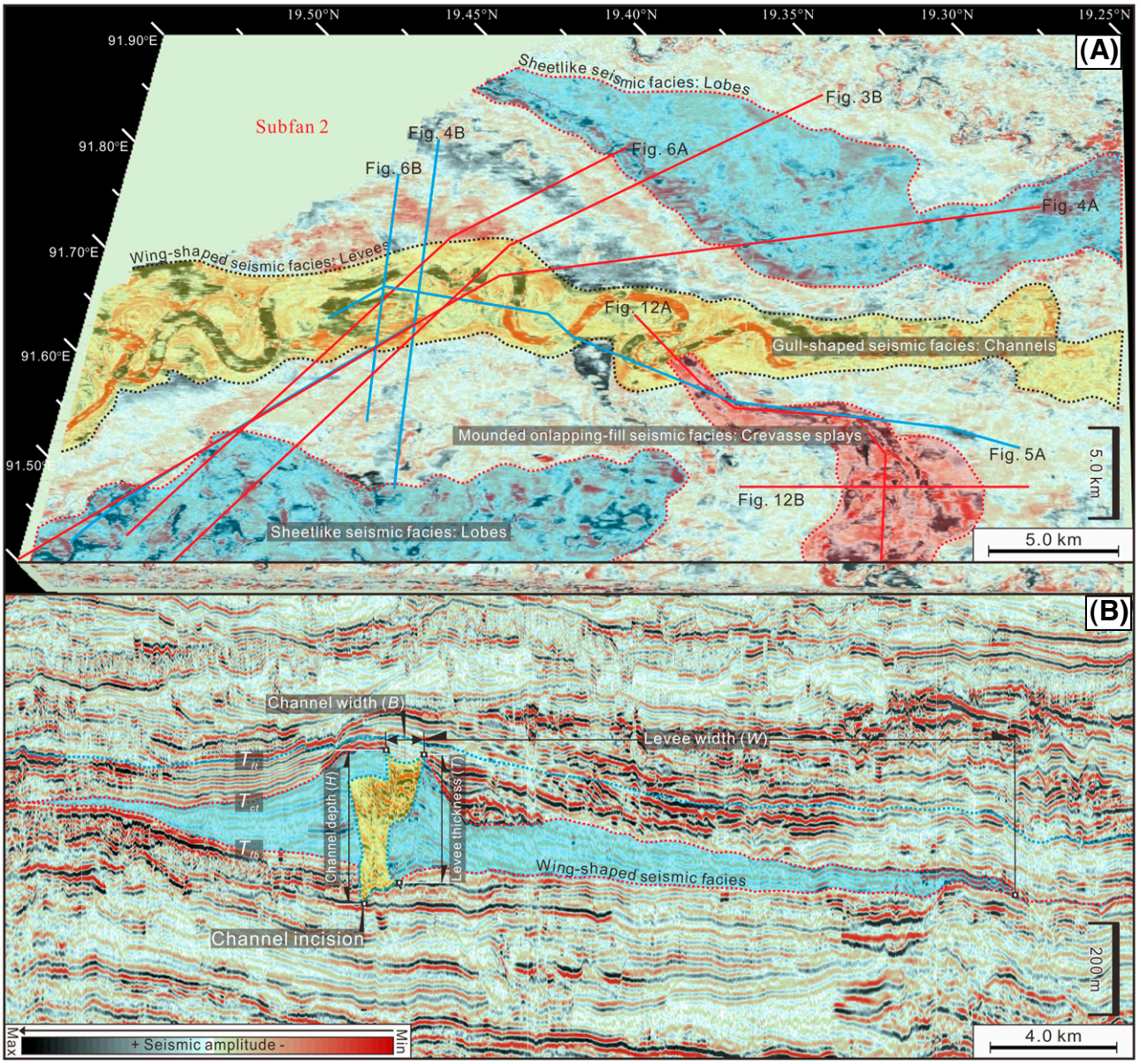

Figure 3. Bengal subfan-growth cycle 2 (subfan 2) as seen (A) on the flattened horizontal seismic amplitude slice and (B) on the strike-view seismic section. Plan-view locations of seismic lines shown in (B) (and in Figures 4; 5A; 6; 12A, B) are shown in (A). T_{ft}, T_{ct}, and T_{fb}, respectively, denote the hanging horizon used to flatten the Bengal three-dimensional seismic database and the upper and basal bounding surfaces of the studied Bengal channel levee complexes. Max = maximum; Min = minimum.

(*W*/*T*)—computed by dividing *W* by *T*. Third, architecture and evolution of the studied channels have been quantified in terms of stratigraphic mobility number (*M*) and angle of channel-complex trajectory (T_c), which are, respectively, defined by (Jerolmack and Mohrig, 2007)

$$M = \frac{dx}{dy}\frac{H}{B} \tag{1}$$

$$T_c = \arctan(dy/dx) \tag{2}$$

where *dx* and *dy* are lateral and vertical components of a specific channel-growth pathway, respectively (see also Jobe et al., 2016). Fourth, architectural styles and growth patterns of the Bengal lobes and crevasse splays are quantified by angle of onlap-point trajectory (T_o), given by

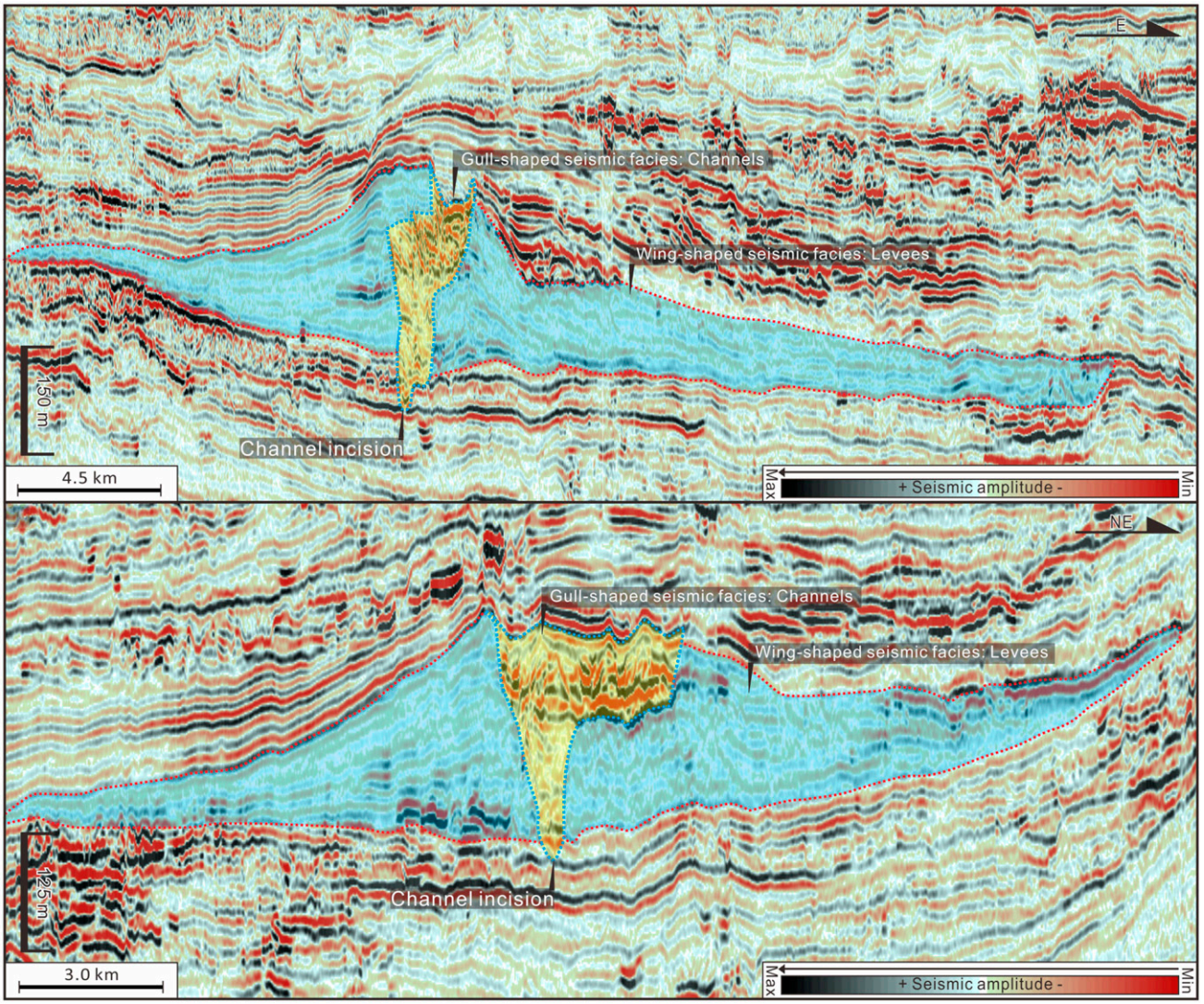

Figure 4. Seismic lines along the depositional strike (line locations shown in Figure 3A) illustrating a cross-sectional seismic view of the Bengal channel levee complexes seen as gull- and wing-shaped seismic facies. Max = maximum; Min = minimum.

$$T_o = \arctan(dy'/dx') \quad (3)$$

where dx' and dy' are lateral and vertical components of a given onlap-point trajectory, respectively (see also Pellegrini et al., 2017).

SEISMIC STRATIGRAPHY AND GEOMORPHOLOGY OF THE BENGAL SUBFANS

In the study interval of interest, three subfan-growth cycles are recognized on the Bengal Fan (Figures 2, 3). Each of them corresponds to a given channel levee–lobe system and consists of four main seismic facies (Figures 3–7). See Table 1 for a complete description and interpretation of these four seismic facies.

Seismic Stratigraphy and Geomorphology of Bengal Channel Levee Complexes

Gull- and Wing-Shaped Seismic Facies

In the cross-sectional view, gull-shaped seismic facies consist of lens-shaped, moderate- to high-amplitude, discontinuous reflectors (Figures 3B, 4, 5A; Table 1). They are bounded at their base by V- to U-shaped basal bounding surfaces and cut deeply into underlying strata (Figures 3B, 4, 5A; Table 1). Gull-shaped seismic facies are collectively flanked by wing-shaped

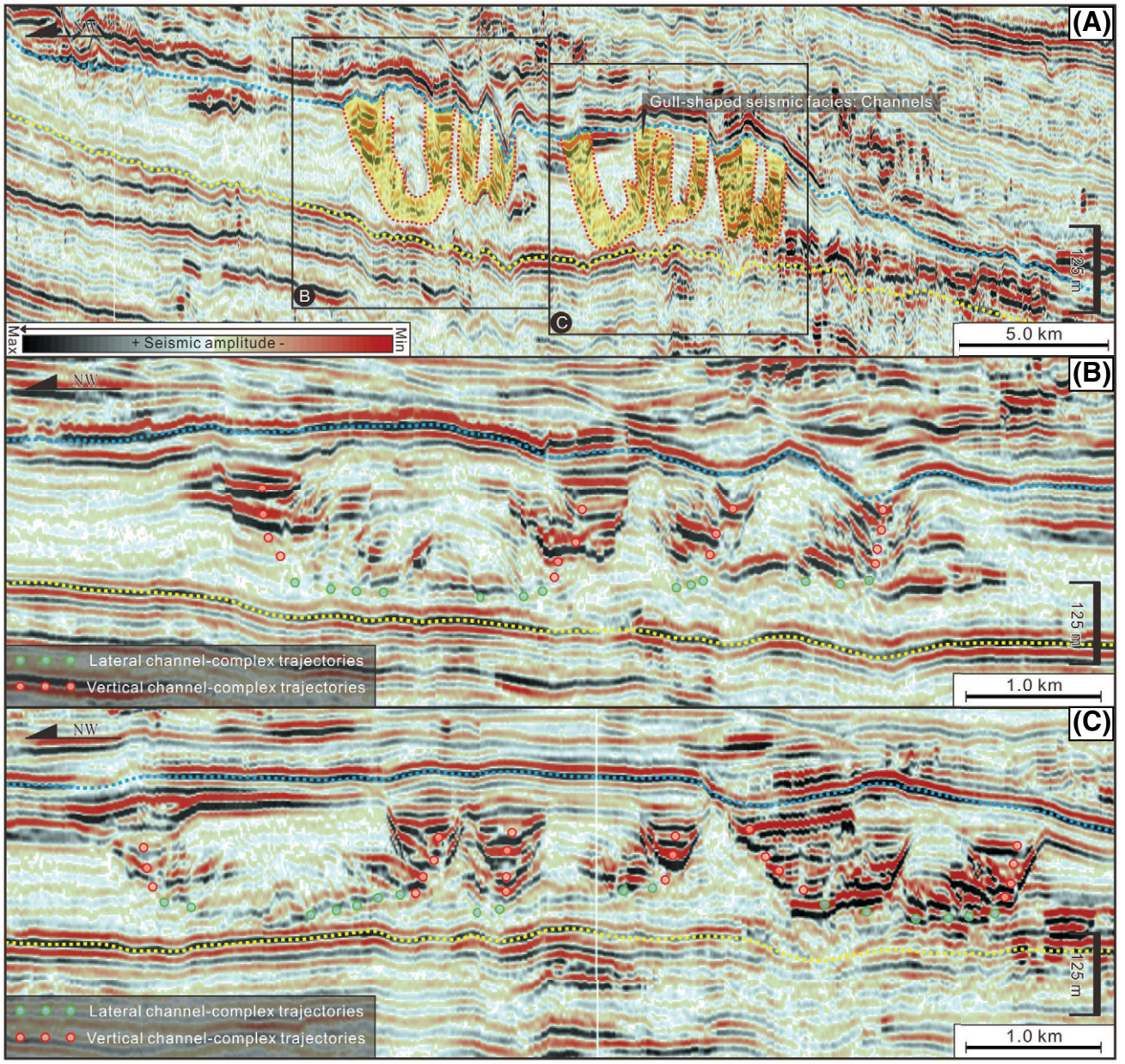

Figure 5. (A) Arbitrary seismic line showing an overall cross-sectional view of the Bengal deepwater channels. Stratigraphic positions of seismic sections shown in (B) and (C) are labeled. (B, C) Seismic transects (see their stratigraphic positions in the black-boxed areas of (A)) showing systematic temporal transition in Bengal channel-complex trajectories from initial lateral migration to subsequent vertical aggradation (green and red circles, respectively). Max = maximum; Min = minimum.

seismic facies that are composed of wedge-shaped, low-amplitude, continuous reflections, forming a typical "gull-wing" seismic signature (Figures 3B, 4, 5A; Table 1). Morphologically, Bengal gull-shaped, seismic facies have bankfull widths (*B*) of 200 to 799 m (averaging 442 m) and bankfull depths (*H*) of 43 to 83 m (averaging 62 m) (Figure 8A), giving rise to an aspect ratio (*B/H*) of 2.94 to 14.22 (averaging 7.29) (Figure 8B). Wing-shaped seismic facies occurring along their flanks are 7.9 to 15.2 m (averaging 12.2 m) in width (*W*) and 154 to 261 m (averaging 224 m) in thickness (*T*) (Figure 9A), resulting in a width-to-thickness ratio (*W/T*) of 46.95 to 59.77 (averaging 54.46) (Figure 9B).

In plan view, the central part of gull-shaped seismic facies is expressed as single, narrow, tortuous, high-amplitude, or high RMS-attribute bands (Figures 3A, 7, respectively; Table 1). Gull-shaped seismic facies show

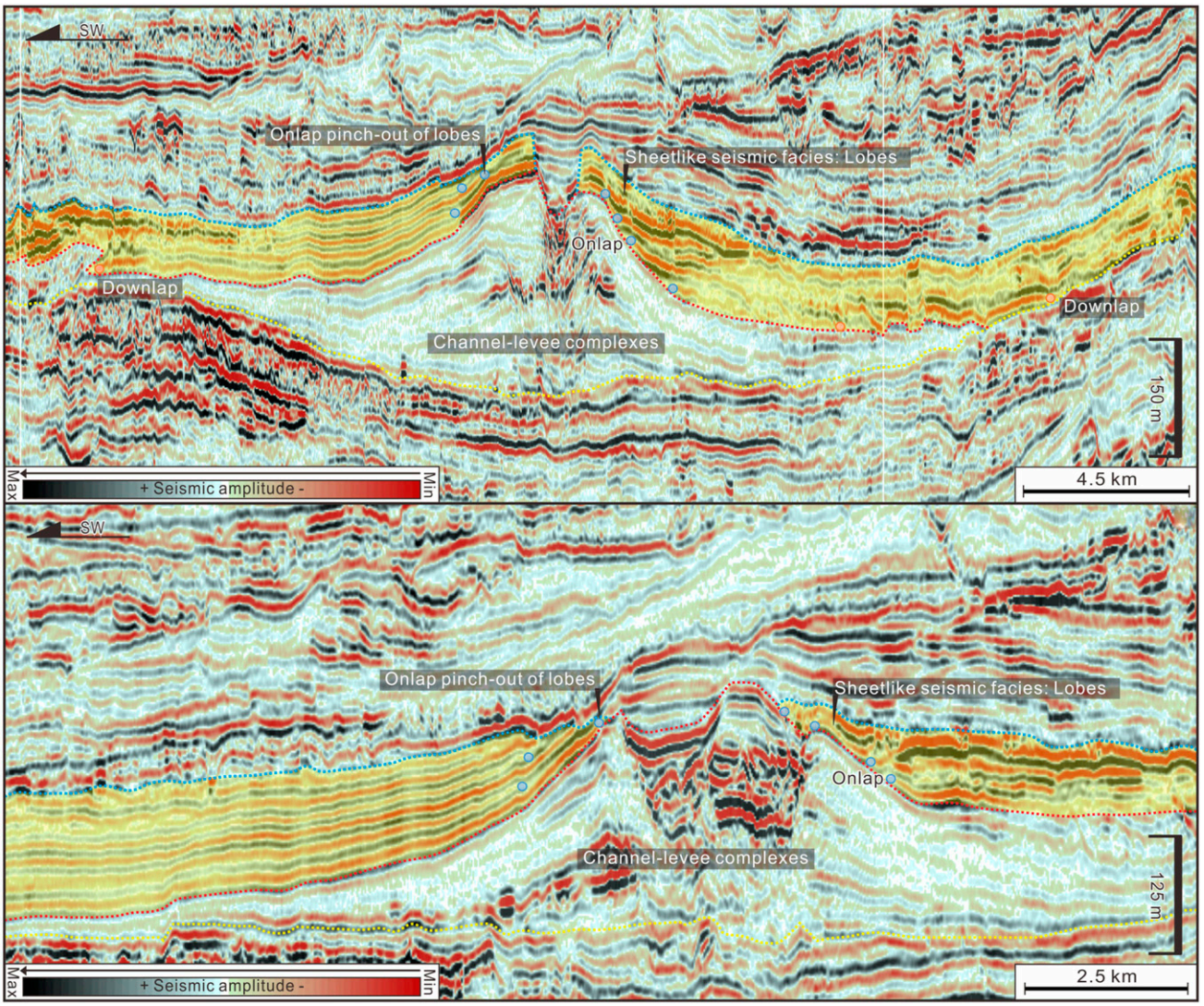

Figure 6. Seismic lines along the depositional strike (line locations shown in Figure 3A) showing cross-sectional seismic manifestations of Bengal lobes recognized as sheet-like seismic facies. The shown Bengal lobes are onlapping the preceding channel levee complexes, resulting in clear onlap-point trajectories and stratigraphic onlap traps. Max = maximum; Min = minimum.

highly sinuous channel courses tens of kilometers long (Figures 3A, 7). Wedge-shaped seismic facies are imaged on plan-view geomorphic images as areally extensive, low-amplitude accumulations (Figure 3A) or low RMS-attribute sheets (Figure 7; Table 1).

Geomorphological Interpretation

Gull-wing seismic signature is commonly taken as the recognition criterion for channel levee complexes on seismic sections (e.g., Janocko et al., 2013; Gong et al., 2015), suggesting that Bengal gull- and wing-shaped seismic facies can be best considered as channel levee complexes (Figures 3, 4, 7; Table 1). Bengal channel levee complexes occur in semiconfined settings (Figure 10A), with thickness ranging from 60 to 90 m (197 to 295 ft) (Figure 10B). These channel levee complexes thin toward the lateral termination of the contemporaneous levees with the thickest deposits occurring along the channel thalweg, thereby showing a progressive decrease in thickness away from the channel thalweg (Figure 10B). As shown in Figure 9A, the scatterplot of levee width (W) against levee thickness (T) suggests that W and T follow a power-law relationship, given as equation 4:

$$T=30.303W^{0.7995} \quad \begin{pmatrix} \text{the coefficient of determination} \\ R^2=0.82,\ n=28 \end{pmatrix} \tag{4}$$

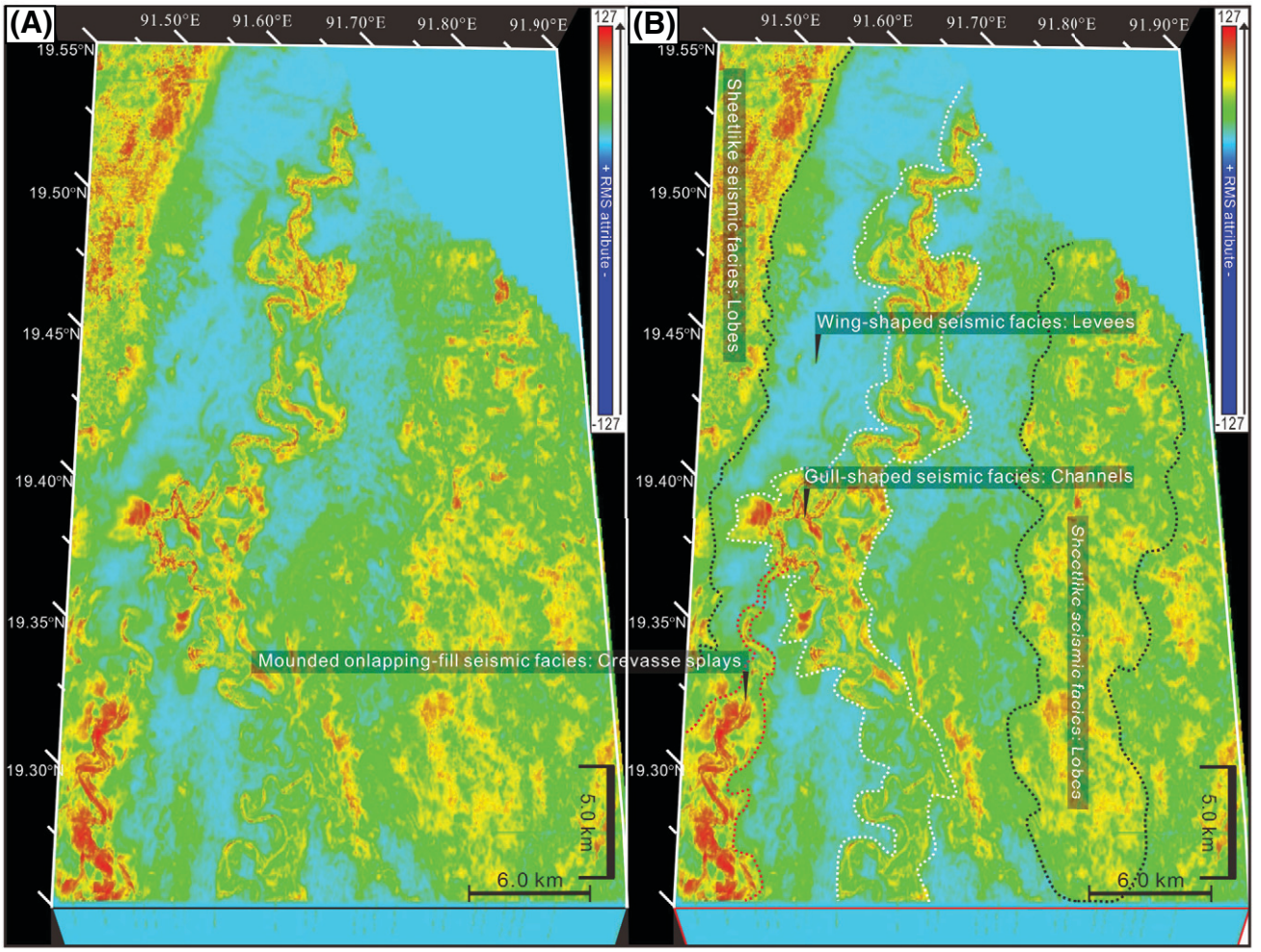

Figure 7. (A) Uninterpreted and (B) interpreted flattened horizontal root-mean-square (RMS)–attribute slices (location shown in Figure 1) showing plan-view geomorphological manifestations of depositional elements associated with Bengal subfan-growth cycle 2, including gull- and wing-shaped seismic facies, sheet-like seismic facies, and mounded onlapping-fill seismic facies.

Seismic Stratigraphy and Geomorphology of Deepwater Lobes

Sheet-Like Seismic Facies

In cross-sectional profile, sheet-like seismic facies are typified by packets of parallel high-amplitude reflectors (Figure 6; Table 1). They are tens to hundreds of meters thick and display tabular cross-sectional geometries (Figure 6; Table 1). Seismic reflectors associated with sheet-like seismic facies occurring along the west sides of the Bengal channel levee complexes (looking downstream) are continuous and consist of uniform amplitude and continuity for a very long distance, whereas those occurring along the east sides of the Bengal channel levee complexes (looking downstream) are slightly disrupted or hummocky in some parts (Figure 6; Table 1).

In plan view, Bengal sheet-like seismic facies occur along both flanks of Bengal channel levee complexes (Figures 3A, 7, 11A). They extend in both dip and strike views for tens of kilometers and occupy an area of up to hundreds of square kilometers (Figures 3A, 4, 5). Bengal sheet-like seismic facies are expressed on the flattened, horizontal, seismic amplitude slices as irregular, high-amplitude accumulations (Figure 3A), and appear on flattened, horizontal, RMS-attribute slices as irregular, high RMS-attribute sheets (Figure 7; Table 1).

Geomorphological Interpretation

Sheet-like seismic facies recognized as packets of parallel, high-amplitude reflections are commonly interpreted to reflect lobes recording the backfilling of the intrachannel lows (Figures 3A, 7, 11A; Table 1)

Table 1. Tabulation of Seismic Facies Descriptions and Interpretations

Seismic Facies	Cross-sectional Seismic Expression			Plan-View Appearance	Seismic Examples	Sedimentological Interpretation
	Amplitude	Continuity	Geometry			
Gull-shaped seismic facies	High	Discontinuous	Lenticular	Single, narrow, tortuous, high-amplitude or high-RMS bands	Figures 3–6, 12	Submarine channels
Wing-shaped seismic facies	Low	Continuous to discontinuous	Wedge-shaped	Irregular low-amplitude or low-RMS accumulations	Figures 3–6	Levees
Sheet-like seismic facies	High to moderate	Continuous to discontinuous	Wedge-shaped	Areally extensive high-amplitude or high RMS-attribute sheets	Figures 4, 9	Deepwater lobes
Mounded onlapping-fill seismic facies	High to moderate	Continuous to discontinuous	Lobate	High-amplitude or high RMS-attribute lobes	Figures 4, 11	Crevasse splays

Abbreviation: RMS = root-mean-square.

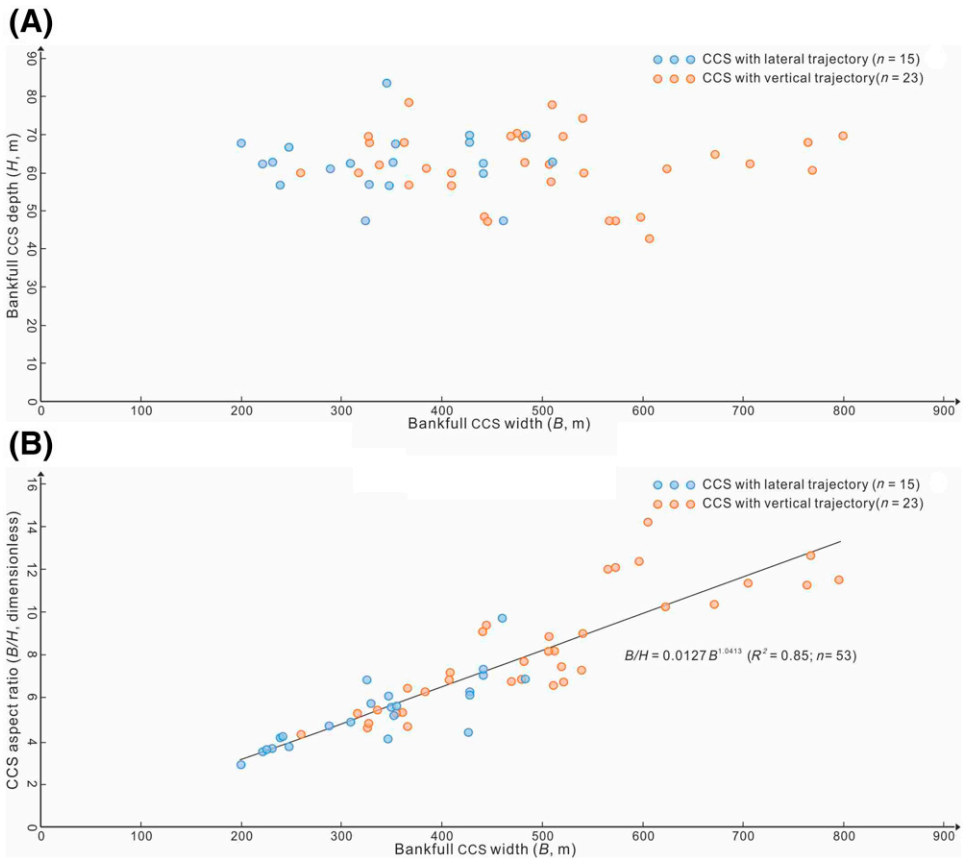

Figure 8. Scatterplots of (A) *B* against *H* and (B) *B* against *B/H* for Bengal deepwater channel-complex sets (CCS) with lateral and vertical trajectories (upper and lower panels, respectively). R^2 = coefficient of determination.

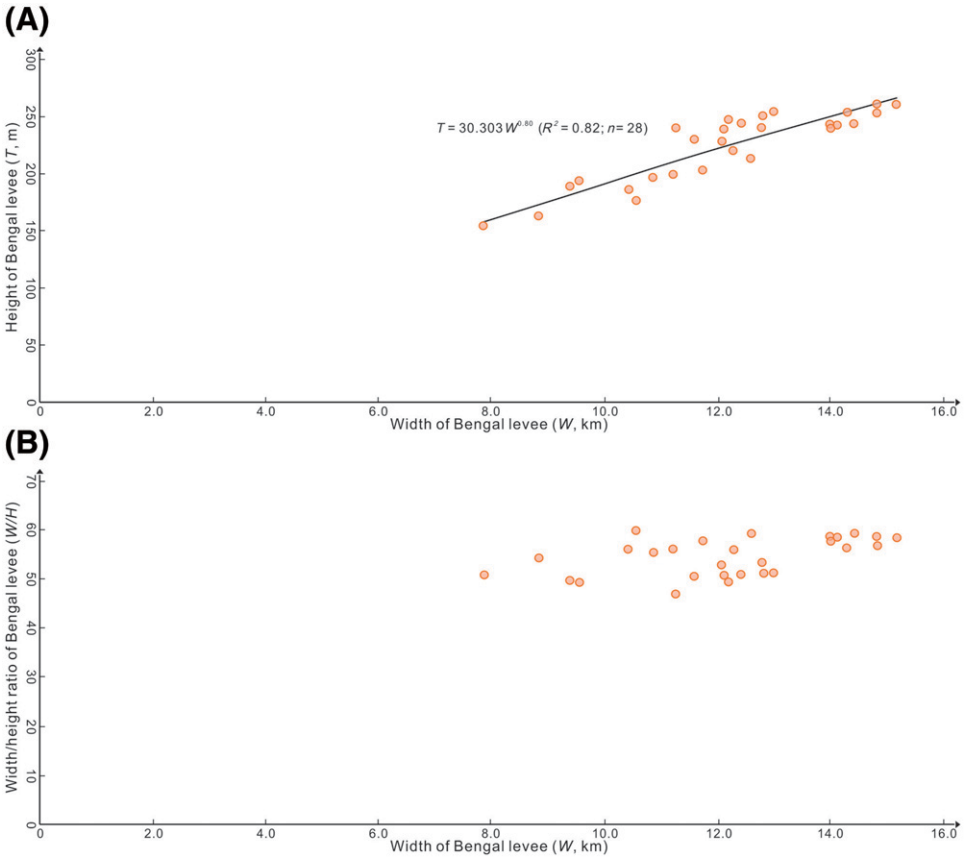

Figure 9. Crossplots of (A) *W* versus *T* and (B) *T* versus *W/T* for levees associated with Bengal deepwater channels. R^2 = coefficient of determination.

(Lopez, 2001; Popescu et al., 2001; Deptuck and Sylvester, 2017). They exhibit a progressive decrease in thickness toward the channel thalweg (i.e., an isopach pattern opposite to that of Bengal channel levee systems) (Figure 10B vs. Figure 11B). Sheet-like seismic facies composed of high-amplitude reflections are also recognized on many other submarine fans worldwide, such as the Amazon (Lopez, 2001), Danube (Popescu et al., 2001), and Astoria Fans (Piper and Normark, 2001). They are commonly seen to occur at the base of channel levee systems and were related to channel avulsions and resultant unchannelized turbidity currents in topographic lows (Lopez, 2001; Deptuck and Sylvester, 2017).

Seismic Stratigraphy and Geomorphology of Crevasse Splays

Mounded Onlapping-Fill Seismic Facies

In depositional dip view, mounded onlapping-fill seismic facies are represented by packets of continuous to discontinuous, high-amplitude reflections and extend for tens of kilometers (Figure 12A; Table 1). They are onlapping onto the preceding channel levee complexes, showing clear onlap-point trajectories (see onlap points marked as blue dots in Figure 12A). In depositional strike view, mounded onlapping-fill seismic facies are typified by packets of moderately continuous, high-amplitude reflections with mounded cross-sectional geometries and extend for hundreds of meters to a few kilometers (Figure 12B; Table 1).

In plan view, mounded onlapping-fill seismic facies were preferentially developed on the external bends of Bengal deepwater channels recognized as gull-shaped seismic facies (Figures 3A, 7, 12). They appear on seismic amplitude volumes as north-south–trending high-amplitude accumulations (Figure 3A) and manifest on 3-D RMS-attribute cubes as lobate-shaped, high RMS-attribute accumulations (Figure 7) (Table 1). Mounded onlapping-fill seismic facies are oblique to the thalweg of the preceding

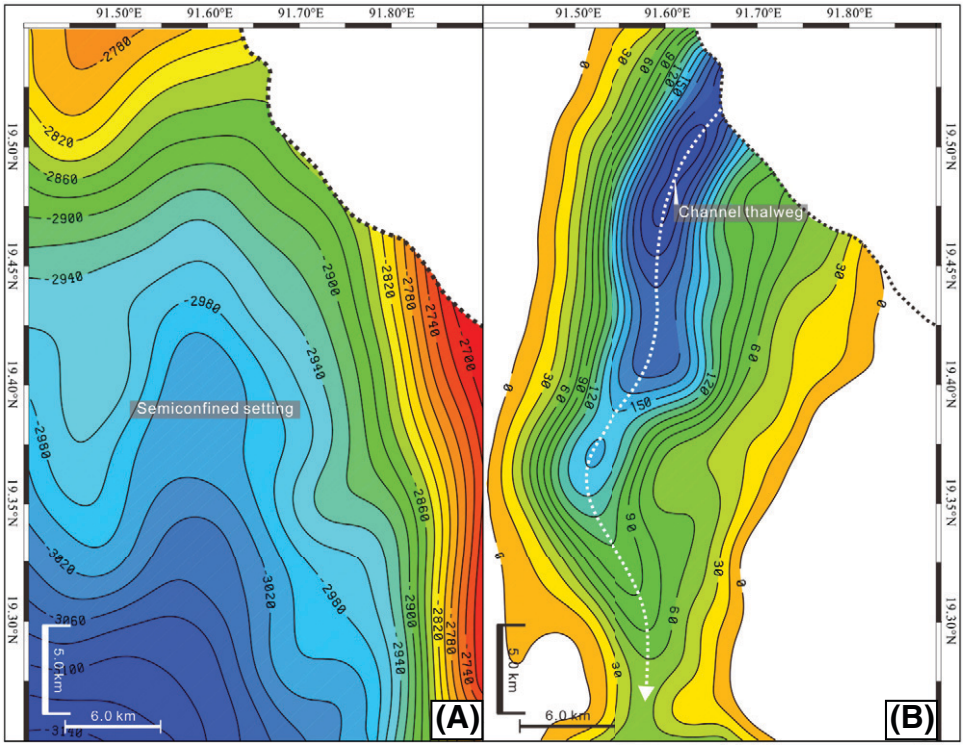

Figure 10. (A) Time-structure map of the basal bounding surface of Bengal channel levee complexes (i.e., T_{fb} in Figure 3B) showing a semiconfined setting for the development of subsequent Bengal channel levee complexes. (B) Isopach map of Bengal channel levee complexes as documented in this case. Colors in (A) and (B), respectively, denote the depth (in milliseconds) and thickness (in meters). Notice the progressive decrease in thickness away from the channel thalweg (i.e., a pattern consistent with the spatial pattern in topographic elevation seen in (A)).

channels seen as gull-shaped seismic facies (Figures 3A, 7). Their plan-view morphology changes upward from lobate to elongate tongue-shaped geometries (Figures 3A, 7). They occupy an area of up to tens of square kilometers and are, thus, volumetrically smaller than Bengal channel levee complexes or lobes (Figures 3A, 7).

Geomorphological Interpretation

Mounded onlapping-fill seismic facies occurring on the external bends of sinuous deepwater channels are commonly interpreted as a body of sediment produced by a spreading, fanning, and collapsing flow originating from a levee breach or crevasse spilling out from a sharp bend of feeder channels (i.e., crevasse splays) (e.g., Posamentier and Kolla, 2003; Lowe et al., 2019). Accordingly, Bengal mounded onlapping-fill seismic facies at the distal end of the channel levee systems are interpreted as the equivalent facies (Figures 3A, 7, 12; Table 1). Bengal crevasse splays preferentially occur in intrachannel lows, in which a lack of confinement most likely results in the deposition of unchannelized turbidity currents formed probably during the initiation of channel avulsion events (Figure 12A).

QUANTIFICATION OF BENGAL SUBFAN GROWTH AND EVOLUTION

The progressive stacking of channels, splays, and/or lobes forms submarine fans (Normark, 1970; Dorrell et al., 2015; Jobe et al., 2017). To understand how Bengal deepwater fans were constructed, it is crucial to quantify repetitive growth patterns of Bengal channel levee complexes, splays, and lobes.

Quantification of Evolution and Growth Patterns of Bengal Channels

Bengal Channel-Complex Trajectories

Architectural styles and growth patterns of the studied channel levee complexes have been quantified by the stratigraphic mobility number (M) and the angle of channel-complex trajectory (T_c). Two discrete

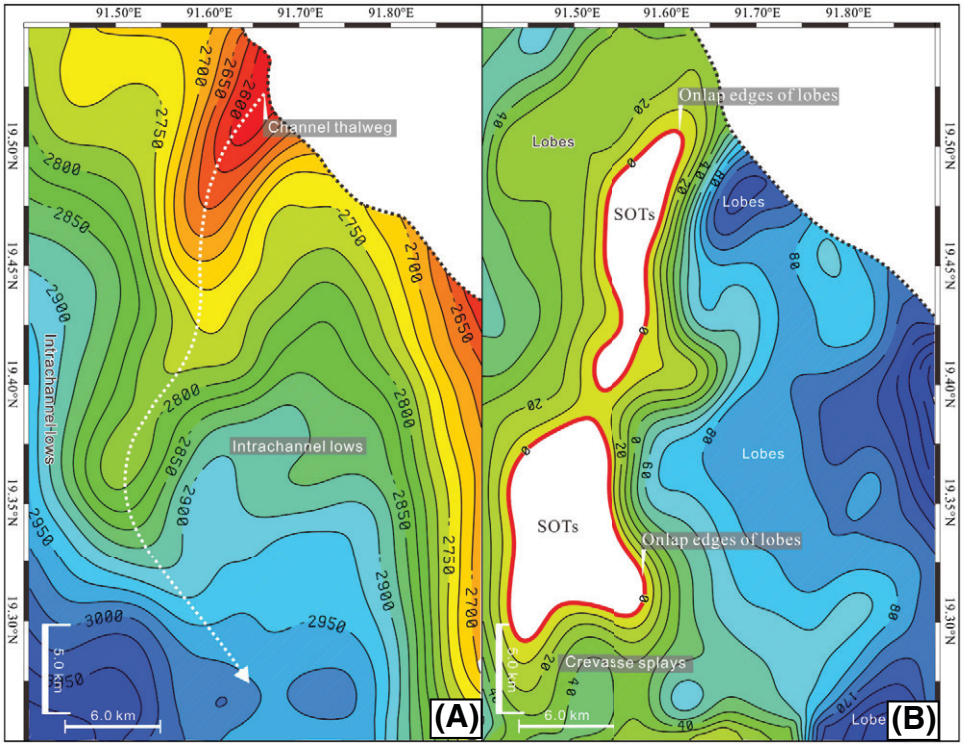

Figure 11. (A) Time-structure map of the upper bounding surface of the Bengal channel levee complexes (i.e., T_{ct} in Figure 3B) showing unconfined settings of intrachannel lows for the development of subsequent lobes and crevasse splays. (B) Isopach map of Bengal lobes and developed during the deposition of Bengal subfan-growth cycle 2. The pinch-out of lobes and splays onto muddy levees created stratigraphic onlap traps (SOTs). Colors in (A) and (B), respectively, denote the depth (in milliseconds) and thickness (in meters). Notice the progressive increase in thickness away from the channel thalweg (i.e., a pattern consistent with the spatial pattern in topographic elevation seen in (A)).

patterns of Bengal channel-complex trajectories are recognized (blue and red dots in Figure 13A, B, respectively). The first population of channel kinematics contains CCSs that have migrated in a dominantly lateral direction (blue dots in Figure 5B, C), thereby displaying a channel kinematic referred to as lateral channel-complex trajectories. Lateral channel-complex trajectories have lateral components (dx) of 144 to 341 m (averaging 205 m) and vertical components (dy) of 4 to 14 m (averaging 8 m), giving rise to relatively low T_c of 1.14° to 4.70° (averaging 2.51°) but to relatively high M of 2.63 to 8.14 (averaging 4.68) (Figure 13A, B).

The second population of channel kinematics is composed of channel complexes that are strongly aggradational and have accreted in a vertical direction through time (orange dots in Figure 13A, B), thereby exhibiting a channel kinematic referred to as vertical channel-complex trajectories. Vertical channel-complex trajectories have dx of 19 to 161 m (averaging 67 m) and dy of 19 to 59 m (averaging 34 m), resulting in relatively high T_c of 10.17° to 57.87° (averaging 30.69°) but relatively low M of 0.06 to 0.93 (averaging M 0.31) (Figure 13A, B).

Twofold Subdivision of Bengal Channel-Complex Trajectories and Stacking Patterns

Lateral channel-complex trajectories are confined within the lower fill level of Bengal channels, whereas vertical channel-complex trajectories seem to be confined within the upper fill level (Figure 13). Bengal channels seen on seismic sections shown in Figure 13 are initially laterally migrating and then return to vertically aggrading, resulting in a twofold trajectory–regime subdivision into younger lateral migration and older vertical aggradation. Previous research on seismic, outcrop, and modeled examples of deepwater channels have also documented the widespread occurrence of such twofold, lateral-vertical trajectory regimes (e.g., Peakall et al., 2000; Labourdette, 2007; Sylvester et al., 2011; Covault et al., 2016; Jobe et al., 2016).

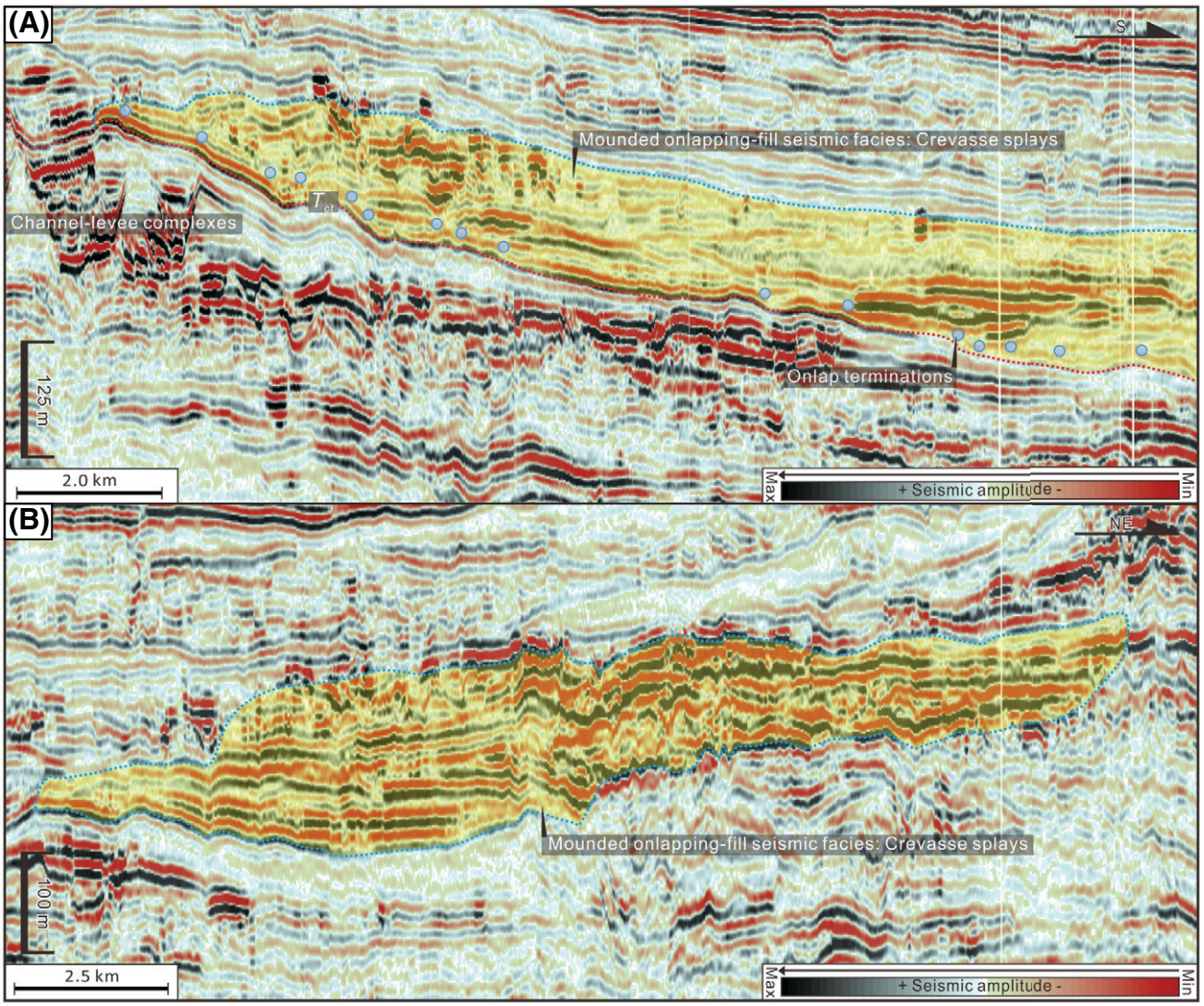

Figure 12. (A) Depositional dip-oriented seismic line (see line locations in Figure 3A) showing the upstream propagation of Bengal crevasse splays. Blue circles shown in (A) denote onlap terminations. (B) Depositional strike-oriented seismic section (see line locations in Figure 3A) showing cross-sectional seismic expression of Bengal crevasse splays. T_{ct} denotes the upper and basal bounding surface of the studied Bengal channel levee complexes. Max = maximum; Min = minimum.

High and low M values are, respectively, indicative of more abundant lateral migration and more abundant vertical channel aggradation (Jobe et al., 2016). According to this assumption, chronologically older Bengal CCSs with a high mean value of $M = 4.68$ and chronologically younger Bengal CCSs with a low mean value of $M = 0.31$ are, respectively, inferred to be abundant in lateral migration (i.e., amalgamation with low aggradation) and in vertical aggradation (i.e., organized stacking with high aggradation) (Figures 5, 13B). Morphologically, laterally amalgamating CCSs have B of 200 to 511 m (averaging 361 m), H of 47 to 83 m (averaging 63 m), and B/H of 2.94 to 9.73 (averaging 5.77) (blue dots in Figure 8A, B). Vertically aggrading CCSs, in contrast, are 259 to 799 m (averaging 500 m) in B, 43 to 79 m (averaging 61 m) in H, and 4.33 to 14.22 (averaging 8.37) in B/H (orange dots in Figure 8A, B). Vertically aggrading CCSs are, thus, two to three times wider than their laterally amalgamating counterparts (Figure 8B).

Quantification of Evolution and Growth Patterns of Bengal Lobes and Splays

Onlap-Point Trajectories of Bengal Lobes and Splays

Submarine lobes recognized as sheet-like seismic facies are onlapping onto the preceding Bengal CCSs,

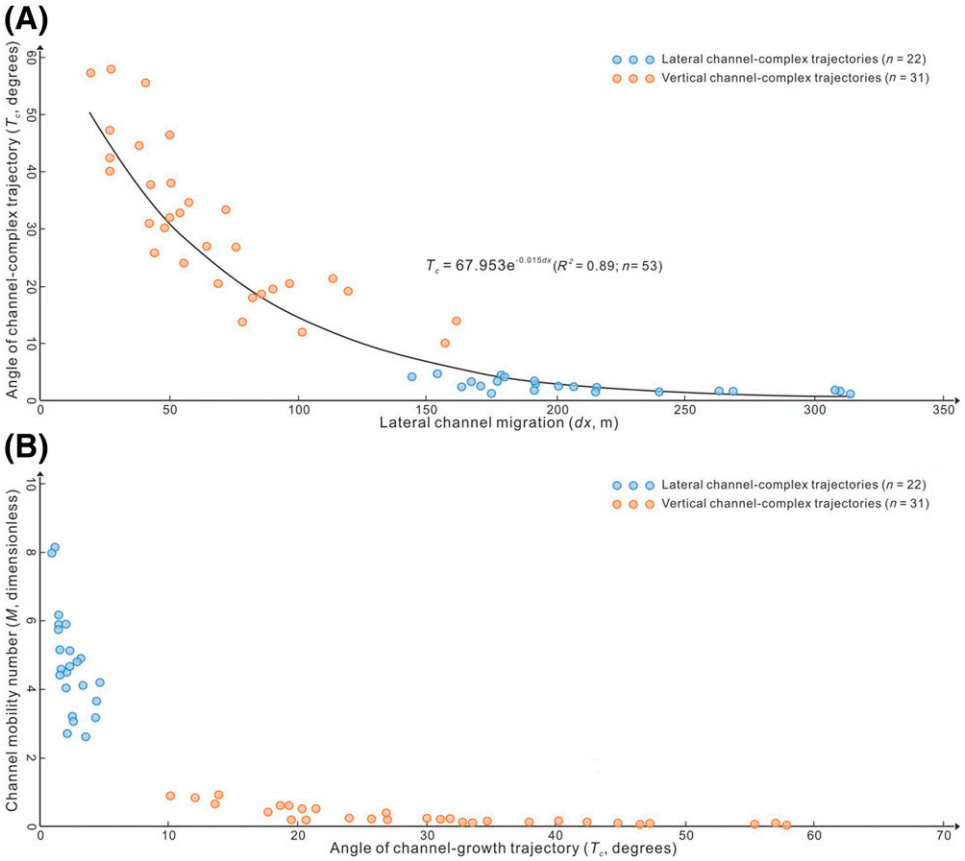

Figure 13. Scatterplots of (A) *dx* against T_c and (B) T_c against *M* for Bengal deepwater channels with lateral and vertical trajectories. R^2 = coefficient of determination.

resulting in lobe onlap-point trajectories (blue dots in Figure 6). Lobe onlap-point trajectories have lateral components of 0.43 to 3.05 km (averaging 1.13 km) and vertical components of 17 to 63 m) (averaging 38 m), giving rise to trajectory angles (T_{bo}) of 1.03° to 3.28°, with a mean value of 2.22° and a standard deviation of ±0.69° (orange dots in Figure 14A, B).

Crevasse splays expressed as mounded onlapping-fill seismic facies are onlapping onto an angular unconformity of T_{ct} (i.e., the upper bounding surface of Bengal channel levee complexes), resulting in lobe onlap-point trajectories (blue dots in Figure 12A). Lobe onlap-point trajectories have lateral components of 0.23 to 1.53 km (0.14 to 0.95 mi) (averaging 0.77 km) and vertical components of 10 to 47 m (averaging 21 m), resulting in trajectory angles (T_{so}) of 0.51° to 3.35°, with a mean value of 1.89° and a standard deviation of ±0.79° (blue dots in Figure 14A, B).

Upstream Propagation of Bengal Lobes and Splays

Bengal lobes are onlapping the preceding Bengal channel levee complexes and display relatively high-angle onlap-point trajectories (reported as T_{bo} of 1.03° to 3.28°, with a mean value of 2.22°) (Figures 6, 14B), pointing to active propagation of lobes. Similarly, Bengal crevasse splays are also onlapping the preceding Bengal channel levee complexes and exhibit rising onlap-point trajectories (having a relatively high angle of 0.51° to 3.35°, with a mean value of 1.89°), also showing active upstream propagation of lobes and splays (Figures 12A, 14B).

GROWTH AND EVOLUTION PATTERNS OF BENGAL SUBFANS

Chronological Order of Bengal Subfan Elements

Three major subfan-growth cycles (subfans 1–3) were recognized in the study interval of interest in the Bengal Fan (Figure 2). Lobes are seen to drape over the channel levee complexes (see onlap terminations indicated by the blue dots in Figure 6) but

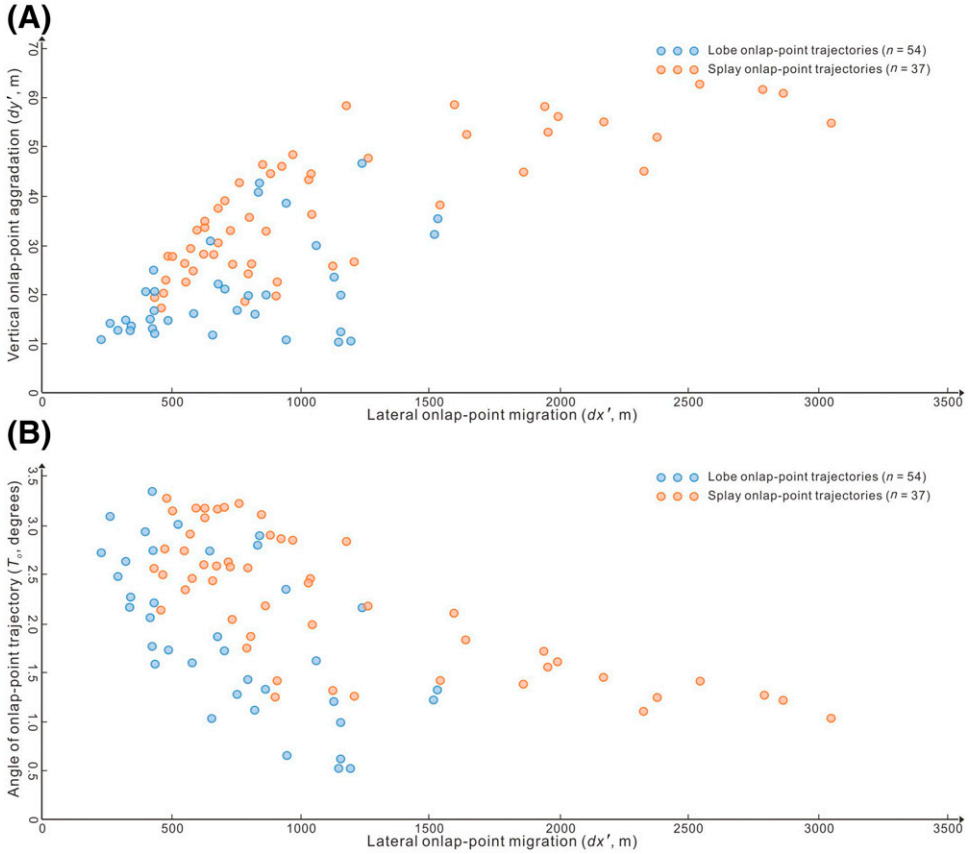

Figure 14. (A) Crossplots of dx' and dy'. (B) Scatterplots of dx' versus T_o.

are onlapping toward the lateral termination of Bengal levees. This, in turn, suggests that lobes are chronologically younger than channel levee complexes. In the same way, crevasse splays are also onlapping toward the thalweg of Bengal channels (Figure 12A), indicating that they are chronologically younger than channel levee systems. However, no stratigraphic relationships between lobes and crevasse splays are seen. This prevents determining the chronological relationship between lobes and crevasse splays. Therefore, the assumption is that lobes and crevasse splays are chronologically synchronous.

Repetitive Patterns of Bengal Subfan Evolution and Growth

This study uses Bengal subfan-growth cycle 2 as an example to explore the evolution and growth patterns of the Bengal Fan at the subfan scale. Our results suggest that a single subfan-growth cycle underwent the following three evolutionary stages (Figure 15): (1) initial channel incision and amalgamation, (2) vertical channel aggradation and resultant creation of intrachannel lows, and (3) channel avulsion and concomitant formation of lobes and splays. Bengal subfan evolutionary stage 1 is recorded by lateral channel-complex trajectories (Figures 5B, C; 15). Stage 2 is illustrated by vertical channel-complex trajectories (Figures 5B, C; 15) and by the presence of intrachannel lows along both flanks of topographic highs as seen on the time-structure map of the upper bounding surface of channel levee complexes (Figure 11A). Bengal subfan evolutionary stage 3 is recorded by onlap-point trajectories of lobes and splays and by changes in thickness of lobes and splays coinciding with the spatial pattern in the topographic elevation of the upper bounding surface of the preceding Bengal channel levee complexes (right versus left panels of Figure 11). These three evolutionary stages constitute a single subfan-growth cycle, which built an individual subfan (i.e., a single channel levee–lobe system) (Figure 15). Typically, an abrupt shift of the channel levee position

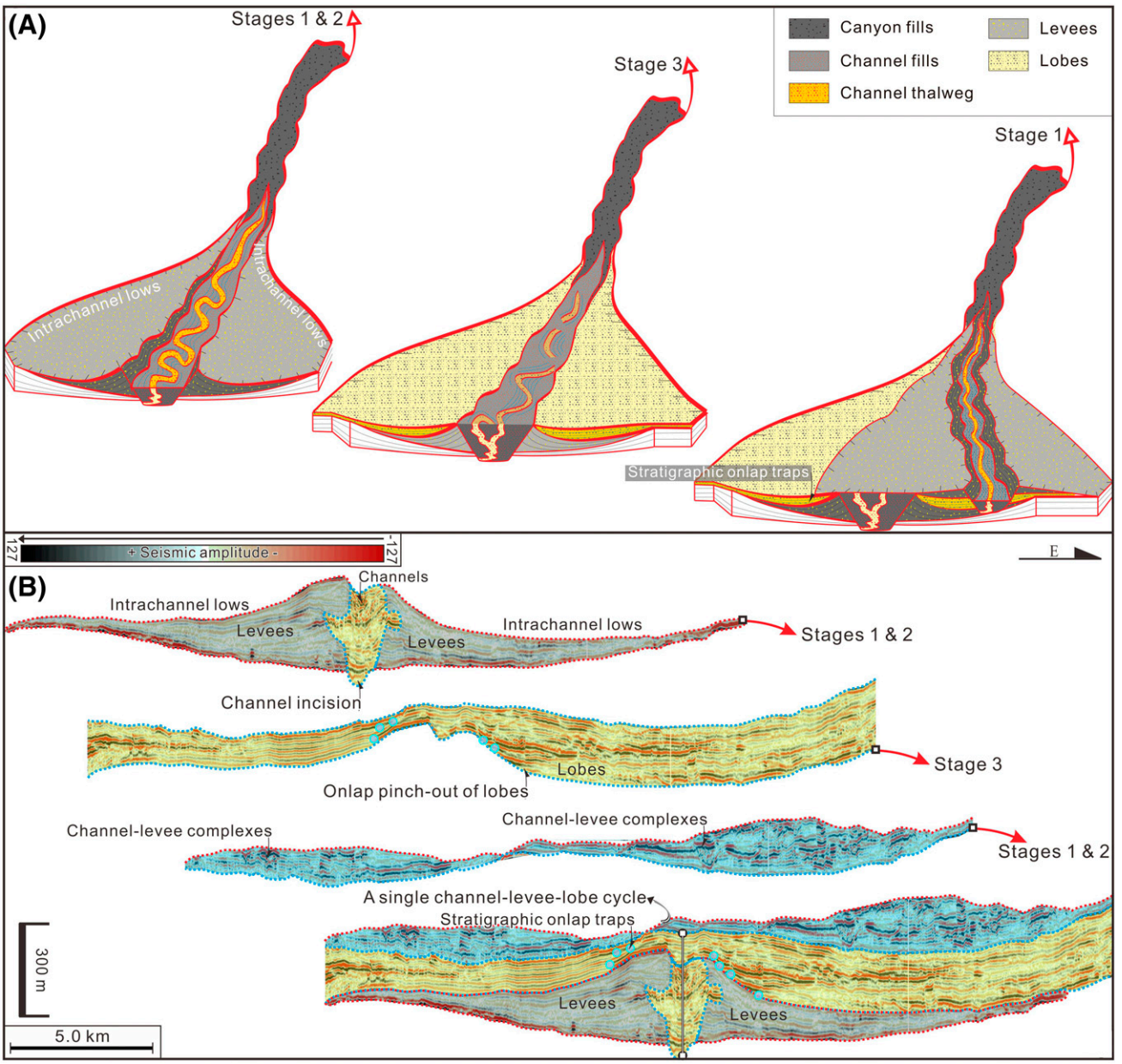

Figure 15. (A) Conceptual model showing how the Bengal Fan grows and evolves at the subfan scale. Note that the pinch-out of lobes and splays onto muddy levees created stratigraphic onlap traps. (B) Seismic transects (line location shown in Figure 3A) illustrating the repetitive patterns of Bengal subfan evolution and growth at the subfan scale. Note that three evolutionary stages constitute a single subfan-growth cycle, which, in turn, led to an individual subfan (i.e., a single channel levee–lobe system).

separates a subfan-growth cycle from the next (Figure 2). Different subfan-growth cycles stacked up over time, giving rise to the world's largest submarine fans in the Bay of Bengal (Figures 2, 15).

IMPLICATIONS

There are two significant implications from the observations and results of the current research. First, the role of autogenic constraints on fan growth and evolution is not well constrained (Lopez, 2001; McHargue et al., 2011; Dorrell et al., 2015). We recognized three individual subfan-growth cycles (subfans 1–3 in Figure 2), which stacked up over time to form the world's largest submarine fan systems in the Bay of Bengal (Figures 2, 15). Our autogenic models of Bengal Fan growth can provide an alternative interpretation of fan growth and evolution that can apply to the predictive models of submarine fan architectures.

Second, industry and academic practitioners witnessed a step change in the volume of oil and gas found in giant stratigraphic and combination traps (Prather, 2003). The central problem with many stratigraphic and combination traps is to make the subtle traps obvious. What is still needed is much better seismic visualization of the reservoirs themselves (Prather, 2003). Our results and observations suggest that stratigraphic pinch-out of lobes and splays onto levees resulting from the subfan-growth stage 3 can serve as lateral trapping elements (see onlap points marked as blue dots in Figure 6 and onlap edges of lobes in Figures 6 and 15). The downlap of subsequent levees onto lateral trapping elements (i.e., sand pinch-outs) most likely act as a competent top seal and prevent hydrocarbons from leaking out, forming stratigraphic onlap traps (Figures 11B, 15B). These stratigraphic onlap traps within intrachannel lows have the potential for large hydrocarbon accumulations (Figures 11B, 15B). They may be common and represent potential drilling targets on many other continental margins worldwide.

CONCLUSIONS

Seismic reflection data from the middle Bengal Fan were used to explore fan growth and evolution at the subfan scale, contributing to a better understanding of fan deposition and stratigraphy. Three subfan-growth cycles were recognized, each of which is represented by an individual channel levee–lobe system and underwent three main evolutionary stages: (1) initial channel incision and amalgamation, (2) vertical channel aggradation and resultant creation of intrachannel lows, and (3) channel avulsion and concomitant propagation of lobes and crevasse splays. Bengal subfan evolution from stages 1 to 2 was recorded by the temporal transition in channel-complex trajectories from lateral migration to subsequent vertical aggradation and the gradual transition in channel stacking patterns from early amalgamation with low aggradation to late-stage organized stacking with high aggradation. Bengal subfan evolution from stages 2 to 3 is documented by onlap-point angles of 0.51° to 3.35° (averaging 2.08°) and by the transition in thickness of lobes and splays coincident with the spatial pattern in topographic elevation. The pinch-out of lobes and splays onto levees developed during subfan-growth stage 3 most likely created stratigraphic onlap traps with the potential for large hydrocarbon accumulations.

REFERENCES CITED

Bastia, R., S. Das, and M. Radhakrishna, 2010, Pre- and post-collisional depositional history in the upper and middle Bengal Fan and evaluation of deepwater reservoir potential along the northeast Continental Margin of India: Marine and Petroleum Geology, v. 27, no. 9, p. 2051–2061, doi:10.1016/j.marpetgeo.2010.04.007.

Bergmann, F., T. Schwenk, V. Spiess, and C. France-Lanord, 2020, Middle to Late Pleistocene architecture and stratigraphy of the lower Bengal Fan—Integrating multichannel seismic data and IODP Expedition 354 results: Geochemistry, Geophysics, Geosystems, v. 21, e2019GC008702, 20 p., doi:10.1029/2019GC008702.

Blum, M., K. Rogers, J. Gleason, Y. Najman, J. Cruz, and L. Fox, 2018, Allogenic and autogenic signals in the sratigraphic record of the deep-sea Bengal Fan: Scientific Reports, v. 8, 7973, 13 p., doi:10.1038/s41598-018-25819-5.

Covault, J. A., 2011, Submarine fans and canyon-channel systems: A review of processes, products, and models: Nature Education Knowledge, v. 3, no. 10, 4.

Covault, J. A., and B. W. Romans, 2009, Growth patterns of deep-sea fans revisited: Turbidite system morphology in confined basins, examples from the California Borderland: Marine Geology, v. 265, no. 1–2, p. 51–66, doi:10.1016/j.margeo.2009.06.016.

Covault, J. A., Z. Sylvester, S. M. Hubbard, Z. R. Jobe, and R. P. Sech, 2016, The stratigraphic record of submarine-channel evolution: The Sedimentary Record, v. 14, no. 3, p. 4–11, doi:10.2110/sedred.2016.3.4.

Curray, J. R., F. J. Emmel, and D. G. Moore, 2002, The Bengal Fan: Morphology, geometry, stratigraphy, history and processes: Marine and Petroleum Geology, v. 19, no. 10, p. 1191–1223, doi:10.1016/S0264-8172(03)00035-7.

Deptuck, M. E., D. J. W. Piper, B. Savoye, and A. Gervais, 2008, Dimensions and architecture of late Pleistocene submarine lobes off the northern margin of east Corsica: Sedimentology, v. 55, no. 4, p. 869–898, doi:10.1111/j.1365-3091.2007.00926.x.

Deptuck, M. E., and Z. Sylvester, 2017, Submarine fans and their channels, levees, and lobes, *in* A. Micallef, S. Krastel, and A. Savini, eds., Submarine geomorphology: Cham, Switzerland, Springer, p. 273–299.

Dorrell, R. M., A. D. Burns, and W. D. McCaffrey, 2015, The inherent instability of leveed seafloor channels: Geophysical Research Letters, v. 42, no. 10, p. 4023–4031, doi:10.1002/2015GL063809.

Galy, V., O. Beyssac, C. France-Lanord, and T. Eglinton, 2008, Recycling of graphite during erosion: A geological stabilization of carbon in the crust: Science, v. 322, no. 5903, p. 943–945, doi:10.1126/science.1161408.

Gong, C., R. J. Steel, K. Qi, and Y. Wang, 2021, Deep-water channel morphologies, architectures, and population densities in relation to stacking trajectories and climate states: Geological Society of America Bulletin, v. 133, no. 1–2, p. 287–306, doi:10.1130/B35431.1.

Gong, C., Y. Wang, D. R. Pyles, R. J. Steel, S. Xu, Q. Xu, and D. Li, 2015, Shelf-edge trajectories and stratal stacking patterns: Their sequence-stratigraphic significance and relation to styles of deep-water sedimentation and amount of deep-water sandstone: AAPG Bulletin, v. 99, no. 7, p. 1211–1243, doi:10.1306/01311513229.

Goodbred, S. L., 2003, Response of the Ganges dispersal system to climate change: A source-to-sink view since the last interstade: Sedimentary Geology, v. 162, no. 1–2, p. 83–104, doi:10.1016/S0037-0738(03)00217-3.

Goodbred, S. L., and S. A. Kuehl, 1999, Holocene and modern sediment budgets for the Ganges-Brahmaputra river system: evidence for highstand dispersal to floodplain, shelf, and deep-sea depocenters: Geology, v. 27, no. 6, p. 559–562, doi:10.1130/0091-7613(1999)027<0559:HAMSBF>2.3.CO;2.

Islam, M. R., S. F. Begum, Y. Yamaguchi, and K. Ogawa, 1999, The Ganges and Brahmaputra rivers in Bangladesh: Basin denudation and sedimentation: Hydrological Processes, v. 13, no. 17, p. 2907–2923, doi:10.1002/(SICI)1099-1085(19991215)13:17<2907::AID-HYP906>3.0.CO;2-E.

Janocko, M., W. Nemec, S. Henriksen, and M. Warchoł, 2013, The diversity of deep-water sinuous channel belts and slope valley-fill complexes: Marine and Petroleum Geology, v. 41, p. 7–34, doi:10.1016/j.marpetgeo.2012.06.012.

Jerolmack, D. J., and D. Mohrig, 2007, Conditions for branching in depositional rivers: Geology, v. 35, no. 5, p. 463–466, doi:10.1130/G23308A.1.

Jobe, Z. R., N. C. Howes, and N. C. Auchter, 2016, Comparing submarine and fluvial channel kinematics: Implications for stratigraphic architecture: Geology, v. 44, no. 11, p. 931–934, doi:10.1130/G38158.1.

Jobe, Z. R., Z. Sylvester, N. Howes, C. Pirmez, A. Parker, A. Cantelli, R. Smith et al., 2017, High-resolution, millennial-scale patterns of bed compensation on a sand-rich intraslope submarine fan, western Niger Delta slope: GSA Bulletin, v. 129, no. 1–2, p. 23–37, doi:10.1130/B31440.1.

Labourdette, R., 2007, Integrated three-dimensional modeling approach of stacked turbidite channels: AAPG Bulletin, v. 91, no. 11, p. 1603–1618, doi:10.1306/06210706143.

Liu, L., T. Zhang, X. Zhao, S. Wu, J. Hu, X. Wang, and Y. Zhang, 2013, Sedimentary architecture models of deep-water turbidite channel systems in the Niger Delta continental slope, West Africa: Petroleum Science, v. 10, no. 2, p. 139–148, doi:10.1007/s12182-013-0261-x.

Lopez, M., 2001, Architecture and depositional pattern of the Quaternary deep-sea fan of the Amazon: Marine and Petroleum Geology, v. 18, no. 4, p. 479–486, doi:10.1016/S0264-8172(00)00071-4.

Lowe, D. R., S. A. Graham, M. A. Malkowski, and B. Das, 2019, The role of avulsion and splay development in deep-water channel systems: Sedimentology, architecture, and evolution of the deep-water Pliocene Godavari "A" channel complex, India: Marine and Petroleum Geology, v. 105, p. 81–99, doi:10.1016/j.marpetgeo.2019.04.010.

Krishna, K. S., J. M. Bull, and R. A. Scrutton, 2009, Early (pre-8 Ma) fault activity and temporal strain accumulation in the central Indian Ocean: Geology, v. 37, no. 3, p. 227–230.

Kudrass, H. R., K. H. Michels, M. Wiedicke, and A. Suckow, 1998, Cyclones and tides as feeders of a submarine canyon off Bangladesh: Geology, v. 26, no. 8, p. 715–718, doi:10.1130/0091-7613(1998)026<0715:CATAFO>2.3.CO;2.

Kuehl, S. A., M. A. Allison, S. L. Goodbred, and H. Kudrass, 2005, The Ganges-Brahmaputra Delta, *in* L. Giosan and J. P. Bhattacharya, eds., River deltas—Concepts, models, and examples: Tulsa, Oklahoma, SEPM Special Publication 83, p. 413–434, doi:10.2110/pec.05.83.0413.

Ma, H., G. Fan, D. Shao, L. Ding, H. Sun, Y. Zhang, Y. Zhang, and B. T. Cronin, 2020, Deep-water depositional architecture and sedimentary evolution in the Rakhine Basin, northeast Bay of Bengal: Petroleum Science, v. 17, p. 598–614, doi:10.1007/s12182-020-00442-0.

McHargue, T., M. J. Pyrcz, M. D. Sullivan, J. D. Clark, A. Fildani, B. W. Romans, J. A. Covault, M. Levy, H. W. Posamentier, and N. J. Drinkwater, 2011, Architecture of turbidite channel systems on the continental slope: Patterns and predictions: Marine and Petroleum Geology, v. 28, no. 3, p. 728–743, doi:10.1016/j.marpetgeo.2010.07.008.

Menard, H. W. Jr., 1955, Deep-sea channels, topography, and sedimentation: AAPG Bulletin, v. 39, no. 2, p. 236–255, doi:10.1306/5CEAE136-16BB-11D7-8645000102C1865D.

Michels, K. H., H. R. Kudrass, C. Hübscher, A. Suckow, and M. Wiedicke, 1998, The submarine delta of the Ganges-Brahmaputra: Cyclone dominated sedimentation patterns: Marine Geology, v. 149, no. 1–4, p. 133–154, doi:10.1016/S0025-3227(98)00021-8.

Michels, K. H., A. Suckow, M. Breitzke, H. R. Kudrass, and B. Kottke, 2003, Sediment transport in the shelf canyon "Swatch of No Ground" (Bay of Bengal): Deep Sea Research Part II: Topical Studies in Oceanography, v. 50, no. 5, p. 1003–1022, doi:10.1016/S0967-0645(02)00617-3.

Mutti, E., and W. R. Normark, 1987, Comparing examples of modern and ancient turbidite systems: Problems and concepts, *in* J. K. Legett and G. G. Zuffa, eds., Marine clastic sedimentology: Dordrecht, the Netherlands, Springer, p. 1–38, doi:10.1007/978-94-009-3241-8_1.

Normark, W. R., 1970, Channel piracy on Monterey deep-sea fan: Deep-Sea Research and Oceanographic Abstracts, v. 17, no. 5, p. 837–846.

Peakall, J., B. McCaffrey, and B. Kneller, 2000, A process model for the evolution, morphology, and architecture of sinuous submarine channels: Journal of Sedimentary

Research, v. 70, no. 3, p. 434–448, doi:10.1306/2DC4091C-0E47-11D7-8643000102C1865D.

Peakall, J., and E. J. Sumner, 2015, Submarine channel flow processes and deposits: A process-product perspective: Geomorphology, v. 244, p. 95–120, doi:10.1016/j.geomorph.2015.03.005.

Pellegrini, C., V. Maselli, F. Gamberi, A. Asioli, K. M. Bohacs, T. M. Drexler, and F. Trincardi, 2017, How to make a 350-m-thick lowstand systems tract in 17,000 years: The Late Pleistocene Po River (Italy) lowstand wedge: Geology, v. 45, no. 4, p. 327–330, doi:10.1130/G38848.1.

Pettingill, H. S., and P. Weimer, 2002, Worldwide deepwater exploration and production: Past, present, and future: The Leading Edge, v. 21, no. 4, p. 371–376, doi:10.1190/1.1471600.

Pickering, J. L., S. L. Goodbred, M. D. Reitz, T. R. Hartzog, D. R. Mondal, and M. S. Hossain, 2014, Late Quaternary sedimentary record and Holocene channel avulsions of the Jamuna and Old Brahmaputra River valleys in the upper Bengal delta plain: Geomorphology, v. 227, p. 123–136, doi:10.1016/j.geomorph.2013.09.021.

Picot, M., L. Droz, T. Marsset, B. Dennielou, and M. Bez, 2016, Controls on turbidite sedimentation: Insights from a quantitative approach of submarine channel and lobe architecture (Late Quaternary Congo Fan): Marine and Petroleum Geology, v. 72, p. 423–446, doi:10.1016/j.marpetgeo.2016.02.004.

Piper, D. J. W., and W. R. Normark, 2001, Sandy fans—From Amazon to Hueneme and beyond: AAPG Bulletin, v. 85, no. 8, p. 1407–1438, doi:10.1306/8626CACD-173B-11D7-8645000102C1865D.

Popescu, I., G. Lericolais, N. Panin, H. K. Wong, and L. Droz, 2001, Late Quaternary channel avulsions on the Danube deep-sea fan, Black Sea: Marine Geology, v. 179, no. 1–2, p. 25–37, doi:10.1016/S0025-3227(01)00197-9.

Posamentier, H. W., and V. Kolla, 2003, Seismic geomorphology and stratigraphy of depositional elements in deep-water settings: Journal of Sedimentary Research, v. 73, no. 3, p. 367–388, doi: 10.1306/111302730367

Prather, B. E., 2003, Controls on reservoir distribution, architecture and stratigraphic trapping in slope settings: Marine and Petroleum Geology, v. 20, no. 6–8, p. 529–545, doi: 10.1016/j.marpetgeo.2003.03.009.

Prélat, A., J. A. Covault, D. M. Hodgson, A. Fildani, and S. S. Flint, 2010, Intrinsic controls on the range of volumes, morphologies, and dimensions of submarine lobes: Sedimentary Geology, v. 232, no. 1–2, p. 66–76, doi:10.1016/j.sedgeo.2010.09.010.

Prélat, A., D. M. Hodgson, and S. S. Flint, 2009, Evolution, architecture and hierarchy of istributary deep-water deposits: A high-resolution outcrop investigation from the Permian Karoo Basin, South Africa: Sedimentology, v. 56, no. 7, p. 2132–2154, doi:10.1111/j.1365-3091.2009.01073.x.

Pyles, D. R., 2008, Multiscale stratigraphic analysis of a structurally confined submarine fan: Carboniferous Ross Sandstone, Ireland: AAPG Bulletin, v. 92, no. 5, p. 557–587, doi:10.1306/01110807042.

Richards, M., M. Bowman, and H. Reading, 1998, Submarine-fan systems I: Characterization and stratigraphic prediction: Marine and Petroleum Geology, v. 15, no. 7, p. 689–717, doi:10.1016/S0264-8172(98)00036-1.

Rogers, K. G., and S. L. Goodbred, 2010, Mass failures associated with the passage of a large tropical cyclone over the Swatch of No Ground submarine canyon (Bay of Bengal): Geology, v. 38, no. 11, p. 1051–1054, doi:10.1130/G31181.1.

Romans, B. W., S. Castelltort, J. A. Covault, A. Fildani, and J. P. Walsh, 2016, Environmental signal propagation in sedimentary systems across timescales: Earth-Science Reviews, v. 153, p. 7–29, doi:10.1016/j.earscirev.2015.07.012.

Schwenk, T., V. Spieb, C. Breitzke, and C. Hübscher, 2005, The architecture and evolution of the Middle Bengal Fan in vicinity of the active channel-levee system imaged by high-resolution seismic data: Marine and Petroleum Geology, v. 22, no. 5, p. 637–656, doi:10.1016/j.marpetgeo.2005.01.007.

Shanmugam, G., 2016, Submarine fans: A critical retrospective (1950–2015): Journal of Palaeogeography, v. 5, no. 2, p. 110–184, doi:10.1016/j.jop.2015.08.011.

Sweet, M. L., and M. D. Blum, 2016, Connections between fluvial to shallow marine environments and submarine canyons: Implications for sediment transfer to deep water: Journal of Sedimentary Research, v. 86, no. 10, p. 1147–1162, doi:10.2110/jsr.2016.64.

Sylvester, Z., C. Pirmez, and A. Cantelli, 2011, A model of submarine channel-levee evolution based on channel trajectories: Implications for stratigraphic architecture: Marine and Petroleum Geology, v. 28, no. 3, p. 716–727, doi:10.1016/j.marpetgeo.2010.05.012.

Weber, M. E., M. H. Wiedicke, H. R. Kudrass, C. Hübscher, and H. Erlenkeuser, 1997, Active growth of the Bengal Fan during sea-level rise and highstand: Geology, v. 25, no. 4, p. 315–318, doi:10.1130/0091-7613(1997)025<0315:AGOTBF>2.3.CO;2.

Yang, S. Y., and J. W. Kim, 2014, Pliocene basin-floor fan sedimentation in the Bay of Bengal (offshore northwest Myanmar): Marine and Petroleum Geology, v. 49, p. 45–58, doi:10.1016/j.marpetgeo.2013.09.007.

Yin, A., 2006, Cenozoic tectonic evolution of the Himalayan orogen as constrained by along-strike variation of structural geometry, exhumation history, and foreland sedimentation: Earth-Science Reviews, v. 76, no. 1–2, p. 1–131, doi:10.1016/j.earscirev.2005.05.004.

Zhang, W., T. Duan, Z. Liu, Y. Liu, L. Zhao, and R. Xu, 2017, Architecture mode, sedimentary evolution and controlling factors of deepwater turbidity channels: A case study of the M Oilfield in West Africa: Petroleum Science, v. 14, p. 493–506, doi:10.1007/s12182-017-0181-2.